

# Reproducing the Acoustic Velocity Vectors in a Circular Listening Area

Jiarui Wang\*, Thushara Abhayapala\*, Jihui Aimee Zhang†, Prasanga Samarasinghe\*  
\*The Australian National University †University of Southampton

March 2024

## Abstract

Acoustic velocity vectors are important for human’s localization of sound at low frequencies. This paper proposes a sound field reproduction algorithm, which matches the acoustic velocity vectors in a circular listening area. In previous work, acoustic velocity vectors are matched either at sweet spots or on the boundary of the listening area. Sweet spots restrict listener’s movement, whereas measuring the acoustic velocity vectors on the boundary requires complicated measurement setup. This paper proposes the cylindrical harmonic coefficients of the acoustic velocity vectors in a circular area (CHV coefficients), which are calculated from the cylindrical harmonic coefficients of the global pressure (global CHP coefficients) by using the sound field translation formula. The global CHP coefficients can be measured by a circular microphone array, which can be bought off-the-shelf. By matching the CHV coefficients, the acoustic velocity vectors are reproduced throughout the listening area. Hence, listener’s movements are allowed. Simulations show that at low frequency, where the acoustic velocity vectors are the dominant factor for localization, the proposed reproduction method based on the CHV coefficients results in higher accuracy in reproduced acoustic velocity vectors when compared with traditional method based on the global CHP coefficients.

## 1 Introduction

Acoustic velocity vectors are the dominant factor for human’s perception of sound at low frequencies, especially below 700 Hz [1,2]. Acoustic velocity vectors are commonly used in Ambisonic encoding and decoding [3,4]. For spatial sound field reproduction system, whose aim is to reproduce a sound field over a region or an area, incorporating acoustic velocity vectors can result in improved perception.

There are multiple ways to incorporate acoustic velocity vectors in spatial sound field reproduction system. First, it is possible to control the acoustic velocity vectors at multiple sweet spots [5]. Sweet spots restricts listener’s movement. Second, based on the Kirchhoff-Helmholtz integral [6], reproduction can be achieved by jointly reproducing the pressure and the acoustic velocity vectors on the boundary of the listening region [7–9]. Measuring the acoustic velocity vectors at multiple control points on the boundary requires complicated and potentially expensive setup, which may not be feasible due to space and financial constraints. Recently, in [10], the spherical harmonic coefficients of the acoustic velocity vectors (SHV coefficients) on the spherical region’s boundary were derived from the spherical harmonic coefficients of the pressure within the region, which can be obtained from spherical microphone array measurements [11,12]. Using a spherical microphone array is easier and possibly cheaper than using multiple velocity probes. Third, the acoustic velocity vectors can be reproduced throughout the listening region, i.e., instead of considering sweet spots or the boundary, the acoustic velocity vectors are reproduced at **every** point inside the listening region.

A spherical region can be modelled as the superposition of spheres with radii that are infinitesimally close to each other. The SHV coefficients in [10] has a radial component. It is possible to match the SHV coefficients at multiple concentric spheres to achieve spatial sound field reproduction. However, the reproduction performance depends on radial sampling, i.e., the selection of the radii of the concentric spheres. In [13], the SHV coefficients independent of the radial distance (SHV-indR) were proposed. The SHV-indR coefficients can be derived from spherical microphone array pressure measurements by using the sound field translation formula. For a spherical region, one set of SHV-indR coefficients is sufficient to model the acoustic velocity

vectors, instead of using multiple sets of SHV coefficients with each set corresponding to a particular radius. The SHV-indR coefficients were used in spatial sound field reproduction and demonstrated better performance at low frequencies when compared with pressure based methods.

This paper builds on [13] and proposes the cylindrical harmonic coefficients of the acoustic velocity vectors (CHV coefficients) in a circular listening area. Like the SHV-indR coefficients, the CHV coefficients are independent of the radial distance. By using the sound field translation formula, the CHV coefficients can be derived from the global CHP coefficients, which are the cylindrical harmonic coefficients of the pressure inside the circular area. The global CHP coefficients can be measured by a circular microphone array. This paper shows that the CHV coefficients can be used in spatial sound field reproduction over two-dimensional space. Moreover, reproduction based on CHV coefficients achieves lower velocity reproduction error when compared with pressure based approach.

## 2 Acoustic velocity vectors in a circular area

### 2.1 The geometric model

Figure 1 shows the setup of the geometric model. This section aims to find the cylindrical harmonic coefficients of the acoustic velocity vectors (CHV coefficients) within the listening area bounded by the blue circle. The derivation first finds the acoustic velocity vector at point  $\mathbf{r}_q$ . The local  $x^{(q)}y^{(q)}z^{(q)}$  coordinate system is the translation of the global  $xyz$  coordinate system with  $\mathbf{r}_q$  as the translation vector. In this paper, the superscript indicates the coordinate system used for expressing the location. When there are no superscripts, the location is expressed using the  $xyz$  coordinate system. For point  $\mathbf{r}$ , the relationship  $\mathbf{r} = \mathbf{r}_q + \mathbf{r}^{(q)}$  holds.

### 3 Acoustic velocity vector at a point

Consider the local region in Figure 1 bounded by the yellow circle. Assume the sound field is height invariant, the pressure at  $\mathbf{r}^{(q)} \equiv (r^{(q)}, \phi^{(q)})$  is

$$p(k, \mathbf{r}^{(q)}) = \sum_{m=-M}^M \alpha_m(k, \mathbf{r}_q) J_m(kr^{(q)}) e^{im\phi^{(q)}} \quad (1)$$

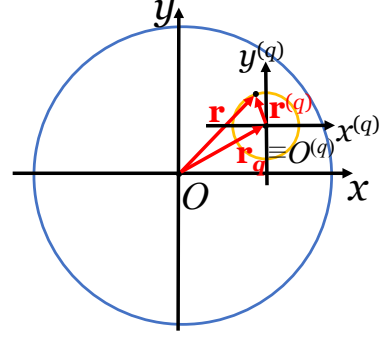


Figure 1: Setup of the geometric model. The listening region is bounded by the blue circle.  $\mathbf{r}_q$  is a point in the listening region.

in which  $\alpha_m(k, \mathbf{r}_q)$  are the cylindrical harmonic coefficients of the local pressure (local CHP coefficients),  $J_m(\cdot)$  is the Bessel function of the first kind and  $M$  is the truncation order. The radial derivative of the Bessel function at the origin satisfies

$$\left. \frac{\partial J_m(kr^{(q)})}{\partial r^{(q)}} \right|_{r^{(q)}=0} = \frac{1}{2}k\delta_{m,1} - \frac{1}{2}k\delta_{m,-1} \quad (2)$$

in which  $\delta_{m,\pm 1}$  are Kronecker delta functions. The acoustic velocity vector at  $\mathbf{r}_q$  is

$$\begin{aligned} V_{\hat{x}}(k, \mathbf{r}_q) &= \left. \frac{i}{k\rho_0c} \frac{\partial p(k, \mathbf{r}^{(q)})}{\partial x} \right|_{r^{(q)}=0} \\ &= \frac{i}{k\rho_0c} \sum_{m=-M}^M \alpha_m(k, \mathbf{r}_q) \left. \frac{\partial J_m(kr^{(q)})}{\partial r^{(q)}} \right|_{r^{(q)}=0} e^{im0} \\ &= \frac{1}{2} \frac{i}{\rho_0c} [\alpha_1(k, \mathbf{r}_q) - \alpha_{-1}(k, \mathbf{r}_q)] \end{aligned} \quad (3)$$

$$\begin{aligned} V_{\hat{y}}(k, \mathbf{r}_q) &= \left. \frac{i}{k\rho_0c} \frac{\partial p(k, \mathbf{r}^{(q)})}{\partial y} \right|_{r^{(q)}=0} \\ &= \frac{i}{k\rho_0c} \sum_{m=-M}^M \alpha_m(k, \mathbf{r}_q) \left. \frac{\partial J_m(kr^{(q)})}{\partial r^{(q)}} \right|_{r^{(q)}=0} e^{im\frac{\pi}{2}} \\ &= -\frac{1}{2} \frac{1}{\rho_0c} [\alpha_1(k, \mathbf{r}_q) + \alpha_{-1}(k, \mathbf{r}_q)] \end{aligned} \quad (4)$$

### 4 Acoustic velocity vector in a circular area

Using the global  $xyz$  coordinate system, the pressure at point  $\mathbf{r} \equiv (r, \phi)$  is

$$p(k, \mathbf{r}) = \sum_{\nu=-V}^V \beta_\nu(k) J_\nu(kr) e^{i\nu\phi} \quad (5)$$

in which  $V$  is the truncation order and  $\beta_\nu(k)$  are the cylindrical harmonic coefficients of the global

pressure (global CHP coefficients). Substituting the sound field translation formula [14]

$$J_\nu(kr)e^{i\nu\phi} = \sum_{m=-\infty}^{\infty} J_{m-\nu}(kr_q)e^{i(\nu-m)(\pi+\phi_q)} J_m(kr^{(q)})e^{im\phi^{(q)}}, \quad (6)$$

into (5), the pressure

$$p(k, \mathbf{r}^{(q)}) = \sum_{m=-M}^M \underbrace{\left[ \sum_{\nu=-V}^V \beta_\nu(k) J_{m-\nu}(kr_q) e^{i(\nu-m)(\pi+\phi_q)} \right]}_{\alpha_m(k, \mathbf{r}_q)} J_m(kr^{(q)}) e^{im\phi^{(q)}}. \quad (7)$$

Let  $n = \nu - m$ ,

$$\alpha_m(k, \mathbf{r}_q) = \sum_{n=-V-m}^{V-m} \beta_{n+m}(k) J_{-n}(kr_q) e^{in(\pi+\phi_q)}. \quad (8)$$

Using the property

$$J_{-n}(\cdot) = (-1)^n J_n(\cdot), \quad (9)$$

equation (8) becomes

$$\alpha_m(k, \mathbf{r}_q) = \sum_{n=-V-m}^{V-m} \underbrace{\beta_{n+m}(k)}_{\gamma_n^{(m)}(k)} J_n(kr_q) e^{in\phi_q} \quad (10)$$

in which  $\gamma_n^{(m)}$  are the cylindrical harmonic coefficients of  $\alpha_m(k, \mathbf{r}_q)$ .

To find the acoustic velocity vector at  $\mathbf{r}_q$ , it is only necessary to calculate  $\alpha_{\pm 1}(k, \mathbf{r}_q)$ , i.e.,  $m = \pm 1$ . To comply with the general form of cylindrical harmonic expansion where the upper summation limit and the lower summation limit are symmetric, (i.e., the summation is of the form  $\sum_{n=-N'}^{N'}$ ), the summation in (10) is truncated to  $\sum_{n=-V+1}^{V-1}$ . From (10), the mapping from  $\beta_\nu(k)$  to  $\gamma_n^{(\pm 1)}(k)$  can be expressed in matrix form

$$\boldsymbol{\gamma}^{(1)}(k) = A^{(1)} \boldsymbol{\beta}(k) \quad (11)$$

$$\boldsymbol{\gamma}^{(-1)}(k) = A^{(-1)} \boldsymbol{\beta}(k) \quad (12)$$

with

$$A^{(1)} = \delta_{n, \nu-1} \quad (13)$$

$$A^{(-1)} = \delta_{n, \nu+1}. \quad (14)$$

The column vectors  $\boldsymbol{\beta}(k) = [\beta_{-V}(k), \dots, \beta_V(k)]^T$  and  $\boldsymbol{\gamma}^{(\pm 1)}(k) = [\gamma_{-V+1}^{(\pm 1)}(k), \dots, \gamma_{V-1}^{(\pm 1)}(k)]^T$ . The matrices  $A^{(1)}$  and  $A^{(-1)}$  are of dimension  $(2V-1)$ -by- $(2V+1)$ . As (13) and (14) suggest,  $A^{(1)}$  and  $A^{(-1)}$  are independent of the wavenumber  $k$ .

Since the acoustic velocity vectors are the linear combinations of  $\alpha_1(k, \mathbf{r}_q)$  and  $\alpha_{-1}(k, \mathbf{r}_q)$ , it is possible to express them using cylindrical harmonic expansion as

$$\mathbf{V}_{\hat{\mathbf{e}}}(k, \mathbf{r}_q) = \sum_{n=-V+1}^{V-1} (\zeta_{\hat{\mathbf{e}}})_n(k) J_n(kr_q) e^{in\phi_q} \quad (15)$$

with  $\hat{\mathbf{e}} \in \{\hat{\mathbf{x}}, \hat{\mathbf{y}}\}$ .  $(\zeta_{\hat{\mathbf{e}}})_n(k)$  are the cylindrical harmonic coefficients of the acoustic velocity vectors (CHV coefficients). Using (3), (4) and the expansion in (10),

$$(\zeta_{\hat{\mathbf{x}}})_n(k) = \frac{1}{2} \frac{i}{\rho_0 c} [\gamma_n^{(1)}(k) - \gamma_n^{(-1)}(k)] \quad (16)$$

$$(\zeta_{\hat{\mathbf{y}}})_n(k) = -\frac{1}{2} \frac{1}{\rho_0 c} [\gamma_n^{(1)}(k) + \gamma_n^{(-1)}(k)]. \quad (17)$$

The mapping from  $\beta_\nu(k)$  to  $(\zeta_{\hat{\mathbf{e}}})_n(k)$  can also be expressed using matrix form

$$\boldsymbol{\zeta}_{\hat{\mathbf{e}}}(k) = A_{\hat{\mathbf{e}}} \boldsymbol{\beta}(k), \quad (18)$$

where

$$A_{\hat{\mathbf{x}}} = \frac{1}{2} \frac{i}{\rho_0 c} [A^{(1)} - A^{(-1)}] \quad (19)$$

$$A_{\hat{\mathbf{y}}} = -\frac{1}{2} \frac{1}{\rho_0 c} [A^{(1)} + A^{(-1)}]. \quad (20)$$

The matrices  $A_{\hat{\mathbf{e}}}$  are of dimension  $(2V-1)$ -by- $(2V+1)$ . If the global CHP coefficients  $\beta_\nu(k)$  are measured up to  $\nu = \pm V$ , the CHV coefficients  $(\zeta_{\hat{\mathbf{e}}})_n(k)$  can be calculated up to order  $n = \pm(V-1)$ . The column vectors  $\boldsymbol{\zeta}_{\hat{\mathbf{e}}}(k) = [(\zeta_{\hat{\mathbf{e}}})_{-V+1}(k), \dots, (\zeta_{\hat{\mathbf{e}}})_{V-1}(k)]^T$ . Moreover, the matrices  $A_{\hat{\mathbf{e}}}$  are independent of the wavenumber  $k$ .

## 5 Illustration of acoustic velocity vectors in a circular area

This section illustrates the acoustic velocity vectors in a circular area when the source is a plane wave and a line source. When the source is a plane wave with incident direction  $\phi_{\text{pw}}$ , using Jacobi-Anger expansion, the global CHP coefficients in (5) are [15]

$$\beta_\nu(k) = i^\nu e^{-i\nu\phi_{\text{pw}}}. \quad (21)$$

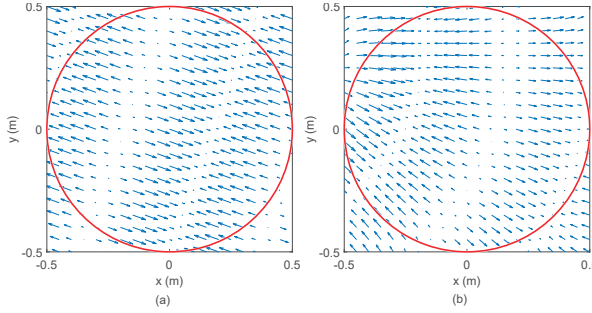


Figure 2: Real part of the acoustic velocity vectors at 500 Hz. (a) The source is a plane wave with incident direction  $\phi_{pw} = 8\pi/9$  rad. (b) The source is a point source at  $\mathbf{r}_s = (1 \text{ m}, 8\pi/9 \text{ rad})$ .

When the source is an infinite line source in  $z$  direction located at  $\mathbf{r}_s \equiv (r_s, \phi_s)$  on the two-dimensional  $xy$  plane, the pressure at  $\mathbf{r} \equiv (r, \phi, z = 0) \equiv (r, \phi)$  can be expressed using (5) and its global CHP coefficients are [16]

$$\beta_\nu(k) = \frac{-i}{4} H_\nu^{(2)}(kr_s) e^{-i\nu\phi_s} \quad (22)$$

in which  $H_\nu^{(2)}(\cdot)$  is the Hankel function of the second kind.

Figure 2 shows the simulation results. The circular area bounded by the red circle has radius 0.5 meters. The global CHP coefficients  $\beta_\nu(k)$  are truncated to order  $\nu = \pm 7$ . Hence, the CHV coefficients  $(\zeta_{\hat{\mathbf{x}}})_n(k)$  are calculated up to order  $n = \pm 6$ . Figure 2(a) illustrates the real part of the acoustic velocity vectors when the source is a plane wave with incident direction  $\phi_{pw} = 8\pi/9$  rad (160 degrees). The acoustic velocity vectors are pointing towards either  $8\pi/9$  rad or  $-\pi/9$  rad. This is because the acoustic velocity vectors of a plane wave are perpendicular to the wave front. Figure 2(b) shows the real part of the acoustic velocity vectors when the source is an infinite line source in  $z$  direction located at  $\mathbf{r}_s = (1 \text{ m}, 8\pi/9 \text{ rad})$  on the two-dimensional  $xy$  plane. The acoustic velocity vectors either diverge from or converge to a point in the direction of  $8\pi/9$  rad. The spherical wave fronts can be discerned.

## 6 Reproducing the acoustic velocity vectors in a circular area

This section highlights the potential of using the CHV coefficients in sound field reproduction system. Reproduction is achieved by matching the desired CHV coefficients using  $L$  number of sources. The reproduction algorithm consists of the record-

ing stage and the reproduction stage. In the recording stage, first, the global CHP coefficients  $\beta_\nu^{(d)}(k)$  of the desired sound field are measured by a circular microphone array. Next, using (18), the desired CHV coefficients  $(\zeta_{\hat{\mathbf{e}}})_n^{(d)}(k)$  with  $\hat{\mathbf{e}} \in \{\hat{\mathbf{x}}, \hat{\mathbf{y}}\}$  are calculated. In the reproduction stage, the first step is to measure the global CHP coefficients  $\beta_\nu^{(\ell)}(k)$  with  $\ell = 1, 2, \dots, L$  in the circular listening area when the input to the  $\ell$ -th source is a unit sinusoidal signal. Next, using (18), the CHV coefficients  $(\zeta_{\hat{\mathbf{e}}})_n^{(\ell)}(k)$  in the circular listening area due to unit sinusoidal input to the  $\ell$ -th source are found. Then, a system of equation is constructed

$$\zeta^{(d)}(k) = \mathbf{H}(k)\mathbf{w}(k). \quad (23)$$

In (23),  $\zeta^{(d)}(k) = [\zeta_{\hat{\mathbf{x}}}^{(d)}(k)^T, \zeta_{\hat{\mathbf{y}}}^{(d)}(k)^T]^T$  in which the column vector  $\zeta_{\hat{\mathbf{e}}}^{(d)}(k)$  is the concatenation of  $(\zeta_{\hat{\mathbf{e}}})_n^{(d)}(k)$ . The matrix  $\mathbf{H}(k) = [\zeta^{(1)}(k), \zeta^{(2)}(k), \dots, \zeta^{(L)}(k)]$ , with its  $\ell$ -th column  $\zeta^{(\ell)}(k) = [\zeta_{\hat{\mathbf{x}}}^{(\ell)}(k)^T, \zeta_{\hat{\mathbf{y}}}^{(\ell)}(k)^T]^T$  in which the column vector  $\zeta_{\hat{\mathbf{e}}}^{(\ell)}(k)$  is the concatenation of  $(\zeta_{\hat{\mathbf{e}}})_n^{(\ell)}(k)$ . The column vector  $\mathbf{w}(k) = [w_1(k), w_2(k), \dots, w_L(k)]$ . Finally, the weight (driving function)  $w_\ell(k)$  of each source is found by solving (23). Suppose the global CHP coefficients  $\beta_\nu^{(d)}(k)$  and  $\beta_\nu^{(\ell)}(k)$  are measured up to  $\nu = \pm V$ , then the dimension of  $\mathbf{H}(k)$  is  $[2 \times (2V - 1)]$ -by- $L$ . This is because the CHV coefficients  $(\zeta_{\hat{\mathbf{e}}})_n^{(d)}(k)$  and  $(\zeta_{\hat{\mathbf{e}}})_n^{(\ell)}(k)$  can only be calculated up to  $n = \pm(V - 1)$ .

This section compares the CHV-based approach with CHP-based approach that matches the global CHP coefficients. In CHP-based approach, a system of equation is constructed

$$\beta^{(d)}(k) = \mathbf{G}(k)\mathbf{w}(k). \quad (24)$$

In (24), the column vector  $\beta^{(d)}(k)$  is formed by concatenating  $\beta_\nu^{(d)}(k)$ . The matrix  $\mathbf{G}(k) = [\beta^{(1)}(k), \beta^{(2)}(k), \dots, \beta^{(L)}(k)]$  in which the  $\ell$ -th column  $\beta^{(\ell)}(k)$  is the concatenation of  $\beta_\nu^{(\ell)}(k)$ . The dimension of  $\mathbf{G}(k)$  is  $(2V + 1)$ -by- $L$ .

Figure 3(a) shows the simulation setup. The loudspeakers are assumed to be infinite line sources in  $z$  direction located on the  $xy$  plane. The five loudspeakers are located on the blue circle of radius 1.5 meters and has azimuth angles  $[0, \pi/4, 3\pi/4, 5\pi/4, 7\pi/4]$  rad. The circular listening area has radius 0.5 meters and is bounded by the red circle. The desired sound field is a plane wave with

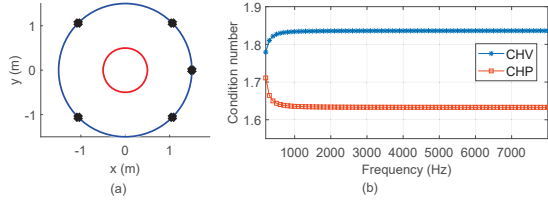


Figure 3: (a) Setup of the reproduction system. The listening area bounded by the red circle has radius 0.5 meters. Black crosses denote loudspeakers. (b) Condition numbers of  $\mathbf{H}(k)$  (CHV-based method) and  $\mathbf{G}(k)$  (CHP-based method).

incident direction  $\phi_{pw} = 8\pi/9$  rad. The global CHP coefficients are truncated to  $\nu = \pm 3$ , which can be measured by a circular microphone array with more than 7 microphones. Hence, the CHV coefficients are truncated to  $n = \pm 2$ . At each wavenumber  $k$ , the dimension of  $\mathbf{H}(k)$  is 10-by-5 and the dimension of  $\mathbf{G}(k)$  is 7-by-5. The condition numbers of  $\mathbf{H}(k)$  and  $\mathbf{G}(k)$  are shown in Figure 3(b). The condition numbers are stable, though those of  $\mathbf{H}(k)$  exceed those of  $\mathbf{G}(k)$ . The loudspeaker weights  $\mathbf{w}(k)$  in (23) and (23) are found by using the Moore-Penrose pseudoinverse, which is calculated by using the `pinv` function in MATLAB with default tolerance. A better tolerance value can be incorporated in future work.

Figure 4 illustrates the reproduced pressure and the acoustic velocity vectors at 500 Hz. Figures 4(a) and 4(c) are from the CHV-based method proposed in this paper, while Figures 4(b) and 4(d) are from the CHP-based method. The ground truth of the acoustic velocity vectors is in Figure 2(a). As in [17] and [18], the velocity reproduction error

$$\epsilon(k) = \cos^{-1}(\text{DOT}(k))/\pi \quad (25)$$

with

$$\text{DOT}(k) = \frac{\mathbf{V}^{(d)}(\mathbf{r}_q, k)}{\|\mathbf{V}^{(d)}(\mathbf{r}_q, k)\|_2} \cdot \frac{\mathbf{V}^{(r)}(\mathbf{r}_q, k)}{\|\mathbf{V}^{(r)}(\mathbf{r}_q, k)\|_2} \quad (26)$$

in which the desired acoustic velocity vector  $\mathbf{V}^{(d)}(\mathbf{r}_q, k) \equiv [V_{\hat{x}}^d(\mathbf{r}_q, k), V_{\hat{y}}^d(\mathbf{r}_q, k)]$  and the reproduced acoustic velocity vector  $\mathbf{V}^{(r)}(\mathbf{r}_q, k) \equiv [V_{\hat{x}}^{(r)}(\mathbf{r}_q, k), V_{\hat{y}}^{(r)}(\mathbf{r}_q, k)]$ . Figure 5 shows the velocity reproduction errors. The blue line and the red line show the velocity reproduction errors averaged across 2821 evaluation points within the red circle of radius 0.5 meters in Figure 3(a). Below 1 kHz, the CHV-based method achieved lower velocity reproduction errors than the CHP method. Above 1 kHz, the CHV-based method and the CHP-based

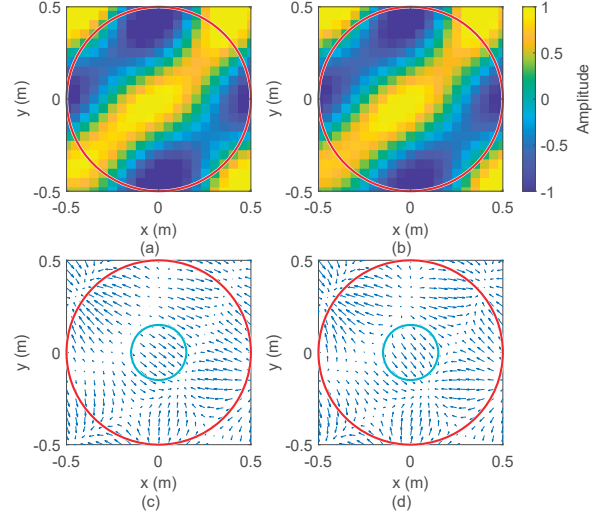


Figure 4: Real part of the reproduced pressure and the reproduced acoustic velocity vectors at 500 Hz. The desired sound field is a plane wave with incident direction  $8\pi/9$  rad. (a) and (c) - CHV-based method; (b) and (d) - CHP-based method.

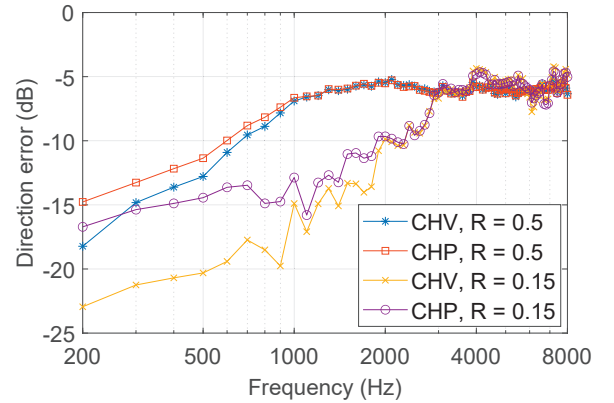


Figure 5: Velocity reproduction errors in the real part of the reproduced acoustic velocity vectors.

method have similar velocity reproduction errors. The yellow line and the purple line illustrate the velocity reproduction errors averaged across 249 evaluation points within the cyan circle of radius 0.15 meters located at the center of the listening region. The improvement due to CHV-based method is more prominent below 1 kHz. The acoustic velocity vectors is most relevant to human's localization of sound at low frequencies [1, 2]. Therefore, this section shows that the CHV-based method could improve localization, when the listener is near the listening region's center. For mid to high frequencies, intensity based reproduction method [3, 18–21] should be considered. Note that the reproduction error will be different when the desired plane wave

is coming from a different direction.

## 7 Conclusion

This paper presented the CHV coefficients, which were the cylindrical harmonic coefficients of the acoustic velocity vectors in a circular area. By using the sound field translation formula, the CHV coefficients were derived from the global CHP coefficients, which were the cylindrical harmonic coefficients of the pressure inside the circular area and could be measured by a circular microphone array. The CHV coefficients were used in sound field reproduction system. Simulation showed that compared with CHP-based method, CHV-based method achieved lower velocity reproduction error at low frequencies, where acoustic velocity vectors are most relevant to human's perception.

## References

- [1] M. A. Gerzon and G. J. Barton, "Ambisonic decoders for HDTV," in *Audio Engineering Society Convention 92*, Mar 1992.
- [2] M. A. Gerzon, "General metatheory of auditory localisation," in *Audio Engineering Society Convention 92*, Mar 1992.
- [3] D. Arteaga, "An ambisonics decoder for irregular 3D loudspeaker arrays," in *The 134th AES Convention*, 01 2013.
- [4] F. Zotter and M. Frank, *Ambisonics: A Practical 3D Audio Theory for Recording, Studio Production, Sound Reinforcement, and Virtual Reality*. Springer, 2019.
- [5] X. Hu, J. Wang, W. Zhang, and L. Zhang, "Time-domain sound field reproduction with pressure and particle velocity jointly controlled," *Applied Sciences*, vol. 11, no. 22, 2021.
- [6] S. Spors, H. Wierstorf, A. Raake, F. Melchior, M. Frank, and F. Zotter, "Spatial sound with loudspeakers and its perception: A review of the current state," *Proceedings of the IEEE*, vol. 101, no. 9, pp. 1920–1938, 2013.
- [7] M. Shin, P. A. Nelson, F. M. Fazi, and J. Seo, "Velocity controlled sound field reproduction by non-uniformly spaced loudspeakers," *Journal of Sound and Vibration*, vol. 370, pp. 444–464, 2016.
- [8] M. Buerger, R. Maas, H. W. Löllmann, and W. Kellermann, "Multizone sound field synthesis based on the joint optimization of the sound pressure and particle velocity vector on closed contours," in *2015 IEEE Workshop on Applications of Signal Processing to Audio and Acoustics (WASPAA)*, 2015, pp. 1–5.
- [9] M. Buerger, C. Hofmann, and W. Kellermann, "Broadband multizone sound rendering by jointly optimizing the sound pressure and particle velocity," *The Journal of the Acoustical Society of America*, vol. 143, no. 3, pp. 1477–1490, 03 2018.
- [10] H. Zuo, T. D. Abhayapala, and P. N. Samarasinghe, "Particle velocity assisted three dimensional sound field reproduction using a modal-domain approach," *IEEE/ACM Transactions on Audio, Speech, and Language Processing*, vol. 28, pp. 2119–2133, 2020.
- [11] T. D. Abhayapala and D. B. Ward, "Theory and design of high order sound field microphones using spherical microphone array," in *2002 IEEE International Conference on Acoustics, Speech, and Signal Processing*, vol. 2, 2002, pp. II–1949–II–1952.
- [12] J. Meyer and G. Elko, "A highly scalable spherical microphone array based on an orthonormal decomposition of the soundfield," in *2002 IEEE International Conference on Acoustics, Speech, and Signal Processing*, vol. 2, 2002, pp. II–1781–II–1784.
- [13] J. Wang, T. Abhayapala, J. A. Zhang, and P. Samarasinghe, "Reproducing the acoustic velocity vectors in a spherical listening region," 2023, arXiv:2307.07200 [eess.AS].
- [14] P. N. Samarasinghe, "Modal based solutions for the acquisition and rendering of large spatial soundfields," Ph.D. dissertation, The Australian National University, 2014.
- [15] M. R. P. Thomas, J. Ahrens, and I. Tashev, "A method for converting between cylindrical and spherical harmonic representations of

- sound fields,” in *2014 IEEE International Conference on Acoustics, Speech and Signal Processing (ICASSP)*, 2014, pp. 4723–4727.
- [16] M. A. Poletti, “Cylindrical harmonic expansion of the sound field due to a rotating line source,” in *Proceedings of 20th International Congress on Acoustics, ICA 2010*, 2010, pp. 211–215.
- [17] L. Birnie, T. Abhayapala, V. Tourbabin, and P. Samarasinghe, “Mixed source sound field translation for virtual binaural application with perceptual validation,” *IEEE/ACM Transactions on Audio, Speech, and Language Processing*, vol. 29, pp. 1188–1203, 2021.
- [18] H. Zuo, P. N. Samarasinghe, and T. D. Abhayapala, “Intensity based spatial soundfield reproduction using an irregular loudspeaker array,” *IEEE/ACM Transactions on Audio, Speech, and Language Processing*, vol. 28, pp. 1356–1369, 2020.
- [19] —, “Intensity based soundfield reproduction over multiple sweet spots using an irregular loudspeaker array,” in *2020 28th European Signal Processing Conference (EUSIPCO)*, 2021, pp. 486–490.
- [20] H. Zuo, T. D. Abhayapala, and P. N. Samarasinghe, “3d multizone soundfield reproduction in a reverberant environment using intensity matching method,” in *ICASSP 2021 - 2021 IEEE International Conference on Acoustics, Speech and Signal Processing (ICASSP)*, 2021, pp. 416–420.
- [21] J.-W. Choi and Y.-H. Kim, “Manipulation of sound intensity within a selected region using multiple sources,” *The Journal of the Acoustical Society of America*, vol. 116, no. 2, pp. 843–852, 08 2004.